RESEARCH ARTICLE | MARCH 12 2024

# Chiral photon emission from a chiral–achiral perovskite heterostructure

Yang Hu ; Ruiwen Chen ; Saloni Pendse; Takashi Taniguchi ; Kenji Watanabe ; Jie Jiang ; Lifu Zhang; Ru Jia; Edmund F. Palermo ; Esther Wertz ; Jian Shi



*Appl. Phys. Lett.* 124, 113301 (2024)
https://doi.org/10.1063/5.0180188

# Chiral photon emission from a chiral–achiral perovskite heterostructure

Cite as: Appl. Phys. Lett. **124**, 113301 (2024); doi: 10.1063/5.0180188
Submitted: 7 October 2023 · Accepted: 25 February 2024 ·
Published Online: 12 March 2024

View Online Export Citation CrossMark

Yang Hu,[1] Ruiwen Chen,[1] Saloni Pendse,[1] Takashi Taniguchi,[2] Kenji Watanabe,[3] Jie Jiang,[1] Lifu Zhang,[1] Ru Jia,[1] Edmund F. Palermo,[1,a)] Esther Wertz,[4,a)] and Jian Shi[1,4,a)]

## AFFILIATIONS

[1]Department of Materials Science and Engineering, Rensselaer Polytechnic Institute, Troy, New York 12180, USA
[2]International Center for Materials Nanoarchitectonics, National Institute for Materials Science, 1-1 Namiki, Tsukuba 305-0044, Japan
[3]Research Center for Functional Materials, National Institute for Materials Science, 1-1 Namiki, Tsukuba 305-0044, Japan
[4]Department of Physics, Rensselaer Polytechnic Institute, Troy, New York 12180, USA

[a)]**Authors to whom correspondence should be addressed:** palere@rpi.edu; wertze@rpi.edu; and shij4@rpi.edu

## ABSTRACT

Chiral semiconductors have been recently suggested as the basic building blocks for the design of chiral optoelectronic and electronic devices for chiral emission and spintronics. Herein, we report that through the formation of a chiral/achiral heterostructure, one can develop a chiral system that integrates the merits of both chiral and achiral components for developing a demanded chiral emitter. In the R-(+)-(or S-(−)-)1-(1-naphthyl)-ethylammonium lead bromide/$CsPbBr_3$ heterostructure, we show that the photoluminescence of $CsPbBr_3$ carries a degree of circular polarization of around 1% at room temperature. It is explained that such chiral emission is enabled through the chiral self-trapped exitonic absorption of R-(+)- (or S-(−)-)1-(1-naphthyl)-ethylammonium lead bromide. This work may provide an alternative way to generate bright circularly polarized light from achiral materials, which has potential applications in spintronics, biosensing, and signal encryption.





Spintronic devices allow active manipulation, transfer, and detection of spin degree of freedom of electrons,[1] which are featured by high computing and storage efficiency[2–6] urgently demanded for future microelectronics and computing paradigms.[7–9] Opto-spintronics, as an emerging branch of spintronics, takes the advantage of the spin of photons (circular polarization of light) to generate and control spin current.[10–12] Chiral materials, matters without mirror symmetry, inversion symmetry, and roto-inversion symmetry, have selective response to left- ($\sigma^-$) and right- ($\sigma^+$) circularly polarized light and can serve as an emitter and a receiver of spin-polarized photons.[13–24] To achieve good performance, chiral semiconductors with large intrinsic chiral response (e.g., circular dichroism), high quantum yield, and suitable bandgap are particularly desirable.[25–30] Low-dimensional hybrid organic–inorganic halide perovskites have high quantum efficiency and can be easily modified to have chirality by selecting chiral organic cation, making them suitable candidates for opto-spintronic devices.[31–47] There are a vast number of chiral perovskite structures designed and discovered in recent years.[38] However, owing to the introduction of bulky organic cations, these chiral organic-inorganic halide perovskites, featured by either Ruddleson–Popper or Dion–Jacobson structures, usually have large bandgap, broad photoluminescence (PL) peak (due to strong electron–phonon coupling), and often lower quantum efficiency at a visible light regime.[33,48–51] One example is organic–inorganic chiral halide perovskite R-(+)- and S-(−)-1-(1-naphthyl)-ethylammonium lead bromide (R- and S-NPB), which not only possesses organic sublattices of chiral $P2_1$ symmetry and helically distorted inorganic framework originating from asymmetric hydrogen bonds but also suffers from dim white photo emission at room temperature.[52]

In this work, we exploit the high brightness visible light emission of pure inorganic halide perovskite $CsPbBr_3$ for a potential chiral emitter through a chiral/achiral heterostructure approach. As shown in Fig. 1, in the heterostructure, we expect to produce an electronic structure that has spin-polarized feature enabling chiral emission. Specifically, we harness the high intrinsic chirality of R- and S-NPB to modify the photoluminescence of $CsPbBr_3$. This approach makes the bright photoluminescence of $CsPbBr_3$ carry reasonable degree of polarization at room temperature. This work may open an avenue for developing a bright chiral emitter for building future chiral optoelectronics.

R- and S-NPB were grown using a solution method.[52] Transparent single crystal (based on visual check) R- and S-NPB crystals in a millimeter size were collected after growth (see Fig. S1 in

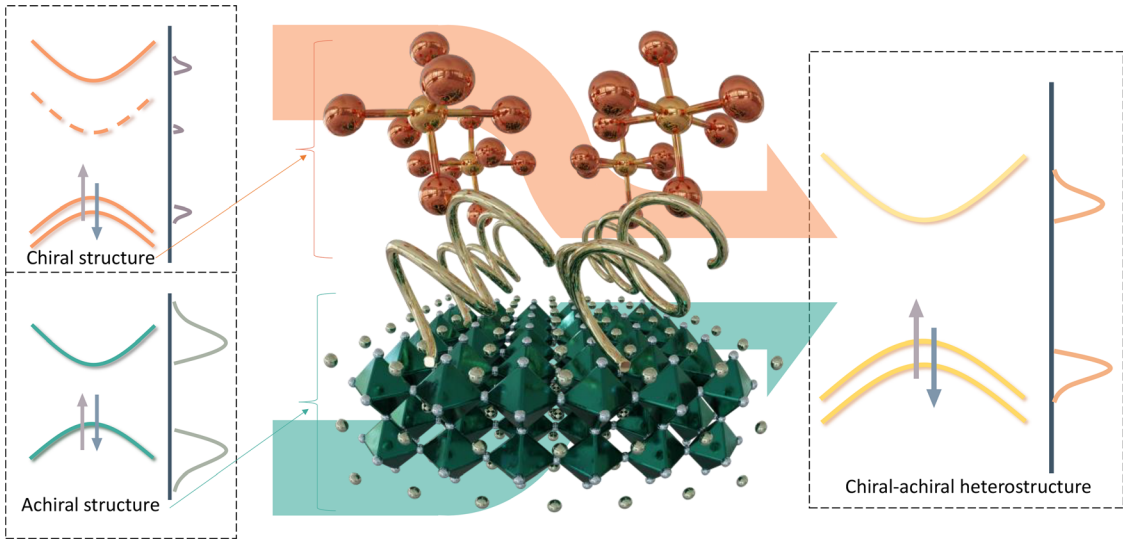


**FIG. 1.** Schematic of a chiral–achiral heterostructure. Van der Waals chiral halide perovskites often have large bandgap and broad PL emission, due to the use of bulky chiral organic cation. 3D perovskites have narrow PL emission and high quantum efficiency but usually possess high symmetry (e.g., no chirality). By building a heterostructure consisting of both chiral van der Waals layer and achiral 3D perovskite, we expect to achieve a narrow and bright PL emission with chirality.

supplementary material). X-ray diffraction (XRD) and nuclear magnetic resonance (NMR) were carried out to verify the phase and chemistry of the synthesized hybrid perovskites, respectively (see Figs. S2 and S3). NPB crystals with a bandgap of 2.97 eV show a weak white PL emission, as shown in Fig. S4, which is attributed to self-trapped exciton owing to strong electron–phonon coupling typically found in low-dimensional hybrid crystals with soft and polar lattice, where lattice anharmonicity leads to spatially localized electron–hole wave functions.[52–54] Time-resolved photoluminescence (TRPL) and temperature-dependent TRPL show (Fig. S5) that the charge carrier lifetimes in NPBs increase with decreasing temperature, from 4 ns (room temperature) to 16 ns (liquid nitrogen temperature) observed at the detection wavelength of 500 nm.

Intrinsic chirality of R- and S-NPB was characterized using a customized setup which extracts circularly polarized luminescence (CPL).[55–57] The CPL experiment setup is shown in Fig. S6. A fixed first polarizer and a rotatable first quarter wave plate (QWP) are used to control polarization of the incident laser. The PL of the device under test is collected by objective lenses and then sent to a charge-coupled device (CCD) after going through a second QWP and a second polarizer. The circular part of PL light was first transformed into linear polarized light by the second rotatable QWP and then modulated by the second fixed polarizer. Specifically, $\sigma^-$ part of PL will be transformed by the second QWP to a linear polarized light with its polarization 45° away from the fast axis of the second QWP, while $\sigma^+$ part of PL will be converted to a linear polarized light with its polarization −45° away from the fast axis. During the rotation of the second QWP, the angle between its fast axis and the polarization direction of the second polarizer keeps changing. When this angle reaches special values like 45° (or 135°), the second polarizer completely blocks the $\sigma^-$ ($\sigma^+$) part of PL, and hence the counts read on CCD will only reflect the contributions from $\sigma^+$ ($\sigma^-$) part of PL. Before experiments, the system is carefully aligned and calibrated using both standard optical mirrors and racemic-NPB (rac-NPB) to quantify the effects of the microscopic components on light modulation (Fig. S7). The polarization direction of the second polarizer and the fast axis of the second QWP are aligned along the same direction prior to tests. During experiments, the rotation angle of QWP is, thus, the angle between the fast axis of the second QWP and polarization direction of the second polarizer.

Figures 2(a)–2(f) show the CPL results of R- and S-NPB with linearly polarized excitation at 405 nm. In Figs. 2(a) and 2(b), CCD readings vs the rotation angle of the second QWP at two different PL wavelengths (442 and 488 nm, respectively) for two periods (360°) are shown. As discussed above, when the rotation angle of the second QWP reaches 45° or 225°, CCD readings represent $\sigma^+$ part of PL; when QWP reaches 135° or 315°, CCD counts represent $\sigma^-$ part of PL. It is clear that at both 442 nm [Fig. 2(a)] and 488 nm [Fig. 2(b)], the PL intensity corresponding to the $\sigma^-$ part in R-NPB is higher than $\sigma^+$, while this is opposite to S-NPB. This is typically seen in chiral materials, as chiral symmetry allows magnetic and electrical dipole moment operators follow same irreducible representation and hence enables selective absorption/emission to photons with different spin.[58,59] In Figs. 2(c) and 2(d), continuously measured results from nine consecutive periods are shown. Here, data are only collected when the rotation angle of the second QWP is equal to 45 plus multiples of 90°. These data show that when the PL is collected at both 527 nm [Fig. 2(c)] and 558 nm [Fig. 2(d)], PL of R-NPB has more $\sigma^-$ component and PL of S-NPB has more $\sigma^+$ part. It is noted that a linear background is intentionally removed in Figs. 2(c) and 2(d) as it may come from graduate laser damage of the sample. Normalized CPL intensity $(I_R-I_L)/(I_R-I_L)_{\mathrm{Max}}$ (here, $I_L$ is the intensity of left circularly polarized PL and $I_R$ is the intensity of right circularly polarized PL) is drawn in Fig. 2(e). R- and S-NPB show opposite CPL values, and we can conclude that R- and S-NPB have evident opposite chirality arising from the chirality of their enantiomorphic organic cations. The degree

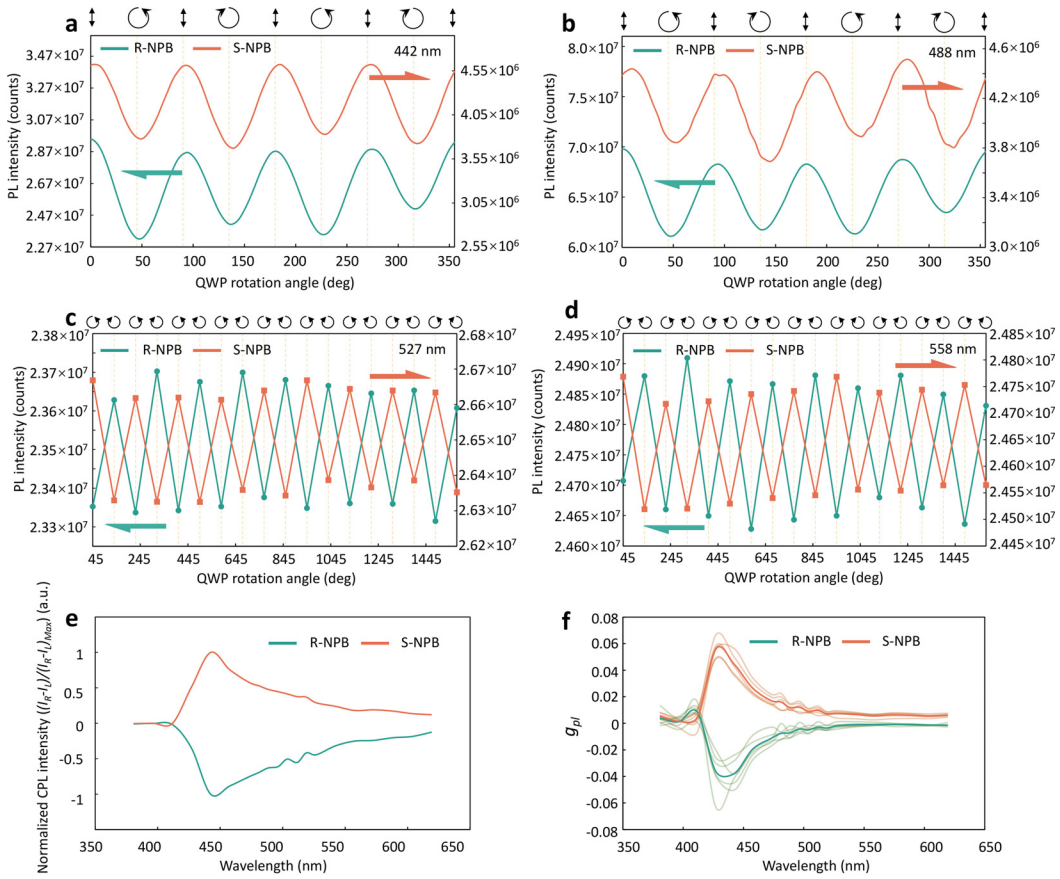


**FIG. 2.** CPL of R-/S-NPB with linear polarized excitation. (a) and (b) CPL response of R-/S-NPB at 442 and 488 nm, respectively. The arrows indicate the corresponding y axes. At both wavelengths, R-NPB has more $\sigma^-$ component (light intensity at 135° is larger than that at 45°), while S-NPB has more $\sigma^+$. (c) and (d) Nine consecutive measurement results of R-/S-NPB at 527 and 558 nm, respectively. (e) and (f) Wavelength dependent normalized CPL intensity and $g_{pl}$, respectively. R- and S-NPB show opposite responses, which is reasonable as they are a pair of enantiomers.

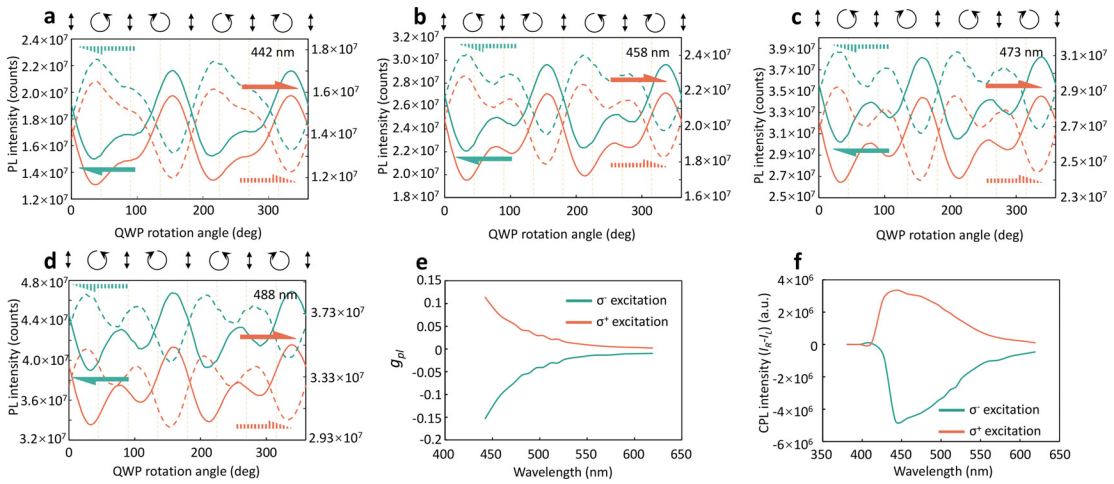


**FIG. 3.** CPL of R-/S-NPB with circularly polarized excitation. (a)–(d) CPL measurement results of R-/S-NPB with $\sigma^-/\sigma^+$ incident light with signals collected at 442, 458, 473, and 488 nm, respectively. Solid lines represent tests with $\sigma^-$ excitation; dashed lines represent $\sigma^+$; green curves represent R-NPB; and red curves represent S-NPB. The arrows indicate the corresponding y axes. (e) and (f) Wavelength dependent $g_{pl}$ factor and CPL intensity of R-NPB. See Fig. S8 for S-NPB.

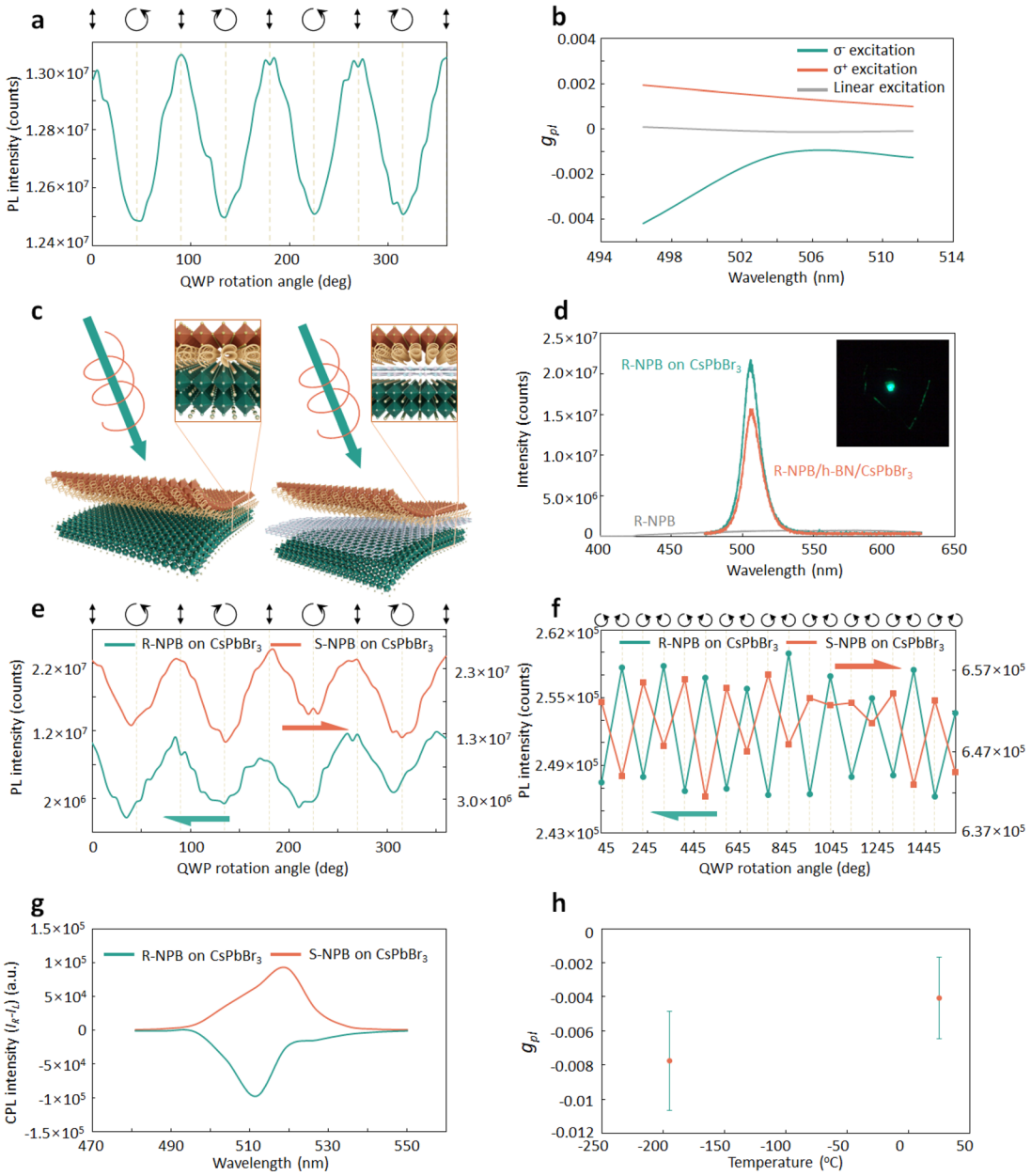


**FIG. 4.** CPL of $CsPbBr_3$ and R- and S-NPB/$CsPbBr_3$/PDMS heterostructures. (a) $CsPbBr_3$ shows no degree of circular polarization with linear excitation. (b) With $\sigma^-/\sigma^+$ excitation, $CsPbBr_3$ shows around −0.4%/0.2% $g_{pl}$. (c) Schematics of two different heterostructures: Left: R- and S-NPB/$CsPbBr_3$/PDMS. Right: R- and S-NPB/h-BN/$CsPbBr_3$/PDMS, where h-BN serves as an insulating layer. (d) PL spectra of our heterostructure and R-NPB perovskite. R-NPB shows a broad weak PL due to its strong electron–phonon coupling. $CsPbBr_3$ possesses strong and sharp green PL owing to its high quantum yield. The heterostructure is dominated by the emission of $CsPbBr_3$. Inset: optical image of R-NPB/$CsPbBr_3$/PDMS heterostructure under excitation. (e) CPL of R- and S-NPB/$CsPbBr_3$/PDMS heterostructure with linearly polarized light as the excitation. The arrows indicate the corresponding y axes. (f) Nine consecutive measurements of CPL. (g) Wavelength dependent CPL intensity. See Fig. S9 for $g_{pl}$ vs wavelength data. (h) $g_{pl}$ of R-NPB/$CsPbBr_3$/PDMS heterostructure at room temperature and liquid nitrogen temperature.

of circular polarization (or luminescence dissymmetry factor) $g_{pl}$ of R- and S- NPB is defined as[60–63]

$$g_{pl} = 2 \times \frac{I_R - I_L}{I_R + I_L}. \quad (1)$$

Figure 2(f) shows $g_{pl}$ vs PL wavelength for both R- and S-NPB. In Fig. 2(f), results from different locations of one sample and different samples are represented in light color, while averaged results are shown in the dark color. With linear illumination at 405 nm, $g_{pl}$ of S- NPB can reach around 6% and R-NPB can reach around −4% both located at ∼450 nm.

Figures 3(a)–3(f) present the CPL results of R- and S-NPB crystals with circularly polarized excitations at 405 nm. Circularly polarized excitations are achieved by rotating the first QWP so that its fast axis is ±45° away from the polarization direction of the first polarizer. In this setup, the $g_{pl}$ is dependent on not only material chirality but also the chirality of incident light, when the spin lifetime of charge carriers is long.[64,65] Under $\sigma^+$ or $\sigma^-$ excitations, CCD counts vs the rotation angle of the second QWP are plotted in Figs. 3(a)–3(d), where solid lines represent results with $\sigma^-$ excitation, dashed lines represent results with $\sigma^+$ excitation, green curves for R-NPB, and red curves for S-NPB. Figures 3(a)–3(d) show measurement results when the PL is at 442, 458, 473, and 488 nm, respectively. It is shown that the $g_{pl}$ is strongly dependent on whether the excitation is $\sigma^+$ or $\sigma^-$, while chirality of the material makes not much difference. Figs. 3(e) and 3(f) present the calculated $g_{pl}$ and CPL intensity ($I_R$-$I_L$) when excitations are $\sigma^+$ and $\sigma^-$, respectively. With $\sigma^-$ illumination, $g_{pl}$ of R- and S-NPB can reach around −15%, while with $\sigma^+$ illumination, $g_{pl}$ can reach around 11%. These results show that the spin lifetime of both R- and S-NPB may be long enough so that the spin states of some excited carriers could reserve through electron–hole recombination.

$CsPbBr_3$ sheets are prepared by a chemical vapor deposition method.[66] After growth, epitaxial rectangle flakes of $CsPbBr_3$ were found on muscovite mica (Fig. S1). As shown in Fig. 4(a), for pure $CsPbBr_3$, with linear excitation, no degree of circular polarization is observed, which is reasonable as $CsPbBr_3$ does not have structural chirality. With $\sigma^-/\sigma^+$ excitation, $CsPbBr_3$ shows a $g_{pl}$ of around −0.4%/0.2%, respectively [Fig. 4(b)], indicating a small portion of excited carriers persevere their original spin states during electron–hole recombination.

R- and S-NPB/$CsPbBr_3$ heterostructures are prepared using a dry transfer method.[67] $CsPbBr_3$ and R- and S-NPB are exfoliated using a Scotch tape and then transferred using polydimethylsiloxane (PDMS). As shown in Fig. 4(c), two different types of devices are prepared: R- and S-NPB/$CsPbBr_3$/PDMS and R- and S-NPB/h-BN/$CsPbBr_3$/PDMS, where h-BN serves as a charge-blocking layer[68,69] (whose purpose will be discussed later). The relevant optical microscopy imagines of these two types of devices are shown in Fig. S10. Although $CsPbBr_3$ has no structural chirality, it has superior quantum efficiency: even with a layer of R-/S-NPB and h-BN on top, its PL intensity is still orders of magnitude larger than that of R-/S-NPB, as shown in Fig. 4(d). Also, PL of $CsPbBr_3$ is a direct emission originating from band-to-band transition, in contrast to the broad self-trapped excitonic PL peak of NPB. By NPB/$CsPbBr_3$ heterostructure, we expect a bright non-chiral emission of $CsPbBr_3$ to be modified by the chirality of NPB.

Figures 4(e)–4(h) show the experimentally received circular polarizations of the PL of R- and S-NPB/$CsPbBr_3$/PDMS heterostructure. Linear polarized excitation at 405 nm is used for these tests. As demonstrated in Fig. 4(e), PL of $CsPbBr_3$ in R- and S-NPB/$CsPbBr_3$/PDMS heterostructures shows certain $g_{pl}$: PL of R-NPB/$CsPbBr_3$/PDMS heterostructure is enriched by $\sigma^-$component, and PL of S-NPB/$CsPbBr_3$/PDMS heterostructure is more populated by $\sigma^+$ component. The signs of $g_{pl}$ are consistent with what have been observed in R- and S-NPB. Figure 4(f) displays the measurement results of nine consecutive periods reflecting the consistency of the degree of circular polarization over different cycles. Wavelength dependent CPL intensity is presented in Fig. 4(g). By forming R-NPB/$CsPbBr_3$/PDMS heterostructure, around −1% $g_{pl}$ is established in PL of $CsPbBr_3$, while around 0.6% $g_{pl}$ is generated by creating S-NPB/$CsPbBr_3$/PDMS heterostructure. At liquid nitrogen temperature, the PL degree of circular polarization increases slightly, as shown in Fig. 4(h).

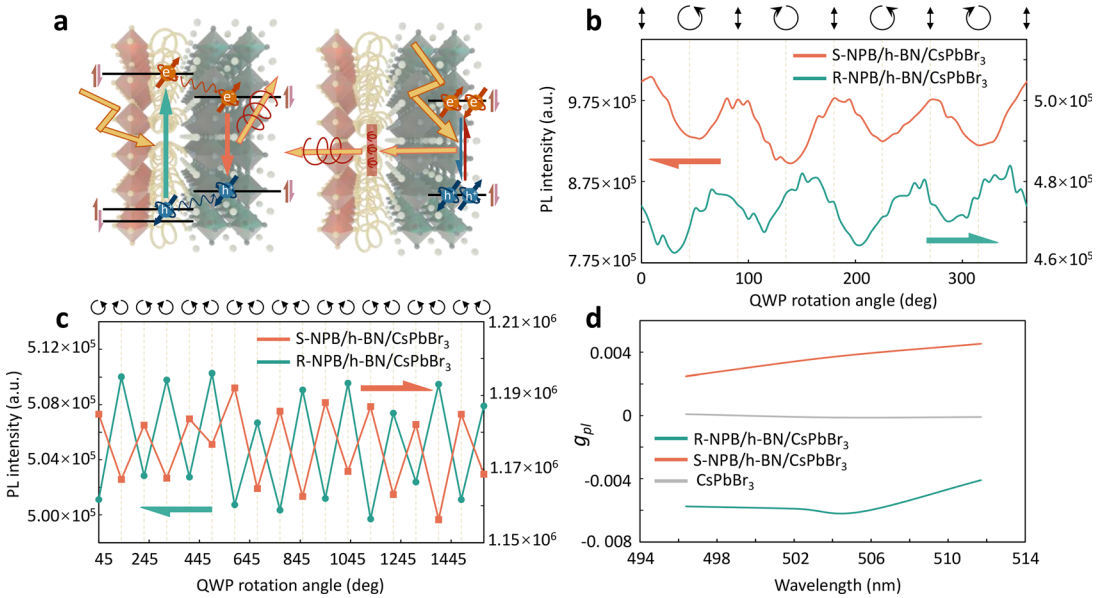


**FIG. 5.** CPL of R- and S-NPB/h-BN/$CsPbBr_3$/PDMS heterostructures. (a), Schematics of two possible mechanisms that may contribute to the chiral emission of our heterostructure. Left: due to material chirality, chiral materials generate spin polarized electron-hole pairs with linearly polarized excitation. Excited electrons and holes diffuse to the achiral layer, and then recombine and emit chiral PL. Right: the chiral layer has different absorption coefficients toward light with different chirality. Hence, it may serve as a "chiral filter" to both incident laser and outcoming PL emission. (b) CPL of R- and S-NPB/h-BN/$CsPbBr_3$/PDMS. Arrows indicate corresponding y axes. (c) CPL of nine consecutive periods. (d) Wavelength dependent $g_{pl}$.

Figure 5(a) shows two possible mechanisms leading to chiral emission from $CsPbBr_3$: first, with linear illumination, chiral materials generate spin polarized electron–hole pairs and then those excited electrons and holes diffuse to a non-chiral layer and further recombine to emit chiral PL;[70,71] second, the chiral layer serves as a "chiral filter" to both incident laser and outcoming emission, owing to its different absorption to $\sigma^-$ and $\sigma^+$ light.[72,73] Hence, a linearly polarized PL beam from the achiral part can be converted to an elliptically polarized light after some circular components are absorbed by the chiral component.

To check whether the first mechanism is possible or not, we insert a layer of h-BN between R-/S-NPB and $CsPbBr_3$ to prevent electron/hole transfer. As shown in Fig. 5(b), even with this layer of h-BN, the PL of $CsPbBr_3$ still shows substantial $g_{pl}$. It is shown that the PL of R-NPB/h-BN/$CsPbBr_3$/PDMS heterostructure at 510 nm has more $\sigma^-$ component, and S-NPB/h-BN/$CsPbBr_3$/PDMS heterostructure has more $\sigma^+$ component, which is consistent with the results of R- and S-NPB and the heterostructures without h-BN. Figure 5(c) show the CPL results for many cycles. The $g_{pl}$ is around –0.6% (0.4%) for R-NPB/h-BN/$CsPbBr_3$/PDMS (S-NPB/h-BN/$CsPbBr_3$/PDMS) heterostructures, which is similar to that of the heterostructures without h-BN [Fig. 5(d)]. These results show that in our heterostructure the mechanism of chiral emission may be dominated by the second one.

In summary, we have demonstrated that by forming a chiral/achiral heterostructure, bright and narrow circularly polarized PL can be obtained. Specifically, the intrinsically high quantum efficiency achiral emission of $CsPbBr_3$ can be tuned to be circularly polarized with $g_{pl}$ at ∼1% at room temperature. We show that this chiral emission mainly comes from the "chiral filtering" effect of the van der Waals chiral perovskite layer. This work opens a door to generate bright chiral emission that could be harnessed for developing future opto-spintronic and quantum computing devices.[74,75]

See the supplementary material synthesis, structural and chemical characterizations, optical measurements, fabrication of heterostructure.

J.S. acknowledges the New York State's Empire State Development's Division of Science, Technology and Innovation through Focus Center Contract No. C180117. J.S. acknowledges the support from the U.S. National Science Foundation under Award Nos. 2024972, 2031692, and 2312944.

## AUTHOR DECLARATIONS

### Conflict of Interest

The authors have no conflicts to disclose.

### Author Contributions

**Yang Hu:** Conceptualization (equal); Data curation (equal); Formal analysis (equal); Validation (equal); Visualization (equal); Writing – original draft (equal). **Ruiwen Chen:** Data curation (equal); Formal analysis (equal); Methodology (equal); Visualization (equal). **Saloni Pendse:** Data curation (equal); Formal analysis (equal); Methodology (equal); Writing – review & editing (equal). **Takashi Taniguchi:** Investigation (equal); Resources (equal). **Kenji Watanabe:** Investigation (equal); Resources (equal). **Jie Jiang:** Data curation (equal); Investigation (equal). **Lifu Zhang:** Data curation (equal); Investigation (equal). **Ru Jia:** Data curation (equal); Formal analysis (equal); Investigation (equal). **Edmund F. Palermo:** Conceptualization (equal); Funding acquisition (equal); Project administration (equal); Supervision (equal); Writing – review & editing (equal). **Esther Wertz:** Funding acquisition (equal); Supervision (equal). **Jian Shi:** Conceptualization (equal); Formal analysis (equal); Funding acquisition (equal); Investigation (equal); Project administration (equal); Supervision (equal); Writing – review & editing (equal).

## DATA AVAILABILITY

The data that support the findings of this study are available from the corresponding authors upon reasonable request.

## REFERENCES

[1]S. A. Wolf and D. Treger, IEEE Trans. Magn. **36**(5), 2748 (2000).
[2]D. D. Awschalom and M. E. Flatté, Nat. Phys. **3**(3), 153 (2007).
[3]J. Puebla, J. Kim, K. Kondou, and Y. Otani, Commun. Mater. **1**(1), 24 (2020).
[4]T. Jungwirth, X. Marti, P. Wadley, and J. Wunderlich, Nat. Nanotechnol. **11**(3), 231 (2016).
[5]F. S. Yasin, J. Masell, K. Karube, D. Shindo, Y. Taguchi, Y. Tokura, and X. Yu, Nat. Commun. **14**(1), 7094 (2023).
[6]O. J. Amin, S. F. Poole, S. Reimers, L. X. Barton, A. Dal Din, F. Maccherozzi, S. S. Dhesi, V. Novák, F. Krizek, J. S. Chauhan, R. P. Campion, A. W. Rushforth, T. Jungwirth, O. A. Tretiakov, K. W. Edmonds, and P. Wadley, Nat. Nanotechnol. **18**(8), 849 (2023).
[7]I. Žutić, J. Fabian, and S. Das Sarma, Rev. Mod. Phys. **76**(2), 323 (2004).
[8]S. D. Bader and S. S. P. Parkin, Annu. Rev. Condens. Matter Phys. **1**(1), 71 (2010).
[9]S. Bhatti, R. Sbiaa, A. Hirohata, H. Ohno, S. Fukami, and S. N. Piramanayagam, Mater. Today **20**(9), 530 (2017).
[10]P. Němec, M. Fiebig, T. Kampfrath, and A. V. Kimel, Nat. Phys. **14**(3), 229 (2018).
[11]J. F. Sierra, J. Fabian, R. K. Kawakami, S. Roche, and S. O. Valenzuela, Nat. Nanotechnol. **16**(8), 856 (2021).
[12]Y. Huang, V. Polojärvi, S. Hiura, P. Höjer, A. Aho, R. Isoaho, T. Hakkarainen, M. Guina, S. Sato, J. Takayama, A. Murayama, I. A. Buyanova, and W. M. Chen, Nat. Photonics **15**(6), 475 (2021).
[13]Y. Hu, F. Florio, Z. Chen, W. A. Phelan, M. A. Siegler, Z. Zhou, Y. Guo, R. Hawks, J. Jiang, J. Feng, L. Zhang, B. Wang, Y. Wang, D. Gall, E. F. Palermo, Z. Lu, X. Sun, T.-M. Lu, H. Zhou, Y. Ren, E. Wertz, R. Sundararaman, and J. Shi, Sci. Adv. **6**(9), eaay4213 (2020).
[14]K. L. Woon, M. O'Neill, G. J. Richards, M. P. Aldred, S. M. Kelly, and A. M. Fox, Adv. Mater. **15**(18), 1555 (2003).
[15]T. Hakkarainen, E. Petronijevic, M. Rizzo Piton, and C. Sibilia, Sci. Rep. **9**(1), 5040 (2019).
[16]H. Lu, J. Wang, C. Xiao, X. Pan, X. Chen, R. Brunecky, J. J. Berry, K. Zhu, M. C. Beard, and Z. V. Vardeny, Sci. Adv. **5**(12), eaay0571 (2019).
[17]D. Li, X. Liu, W. Wu, Y. Peng, S. Zhao, L. Li, M. Hong, and J. Luo, Angew. Chem., Int. Ed. **60**(15), 8415 (2021).
[18]G. Long, C. Jiang, R. Sabatini, Z. Yang, M. Wei, L. N. Quan, Q. Liang, A. Rasmita, M. Askerka, G. Walters, X. Gong, J. Xing, X. Wen, R. Quintero-Bermudez, H. Yuan, G. Xing, X. R. Wang, D. Song, O. Voznyy, M. Zhang, S. Hoogland, W. Gao, Q. Xiong, and E. H. Sargent, Nat. Photonics **12**(9), 528 (2018).
[19]Y. Peng, X. Liu, L. Li, Y. Yao, H. Ye, X. Shang, X. Chen, and J. Luo, J. Am. Chem. Soc. **143**(35), 14077 (2021).
[20]L. Wang, Y. Xue, M. Cui, Y. Huang, H. Xu, C. Qin, J. Yang, H. Dai, and M. Yuan, Angew. Chem., Int. Ed. **59**(16), 6442 (2020).
[21]J. Crassous, M. J. Fuchter, D. E. Freedman, N. A. Kotov, J. Moon, M. C. Beard, and S. Feldmann, Nat. Rev. Mater. **8**(6), 365 (2023).
[22]A. Rauschenbeutel and P. Schneeweiss, Nat. Photonics **16**(4), 261 (2022).
[23]S. Ma, Y.-K. Jung, J. Ahn, J. Kyhm, J. Tan, H. Lee, G. Jang, C. U. Lee, A. Walsh, and J. Moon, Nat. Commun. **13**(1), 3259 (2022).

[24]L. Kang, S. Lan, Y. Cui, S. P. Rodrigues, Y. Liu, D. H. Werner, and W. Cai, Adv. Mater. **27**(29), 4377 (2015).
[25]S.-H. Yang, R. Naaman, Y. Paltiel, and S. S. P. Parkin, Nat. Rev. Phys. **3**(5), 328 (2021).
[26]Y. Deng, M. Wang, Y. Zhuang, S. Liu, W. Huang, and Q. Zhao, Light **10**(1), 76 (2021).
[27]W. Li, M. Xu, C. Ma, Y. Liu, J. Zhou, Z. Chen, Y. Wang, H. Yu, J. Li, and S. Liu, ACS Appl. Mater. Interfaces **11**(26), 23512 (2019).
[28]Y. Dang, X. Liu, B. Cao, and X. Tao, Matter **4**(3), 794 (2021).
[29]J. Ahn, S. H. Lee, I. Song, P. Chidchob, Y. Kwon, and J. H. Oh, Device **1**(5), 100176 (2023).
[30]H. Lu, Z. V. Vardeny, and M. C. Beard, Nat. Rev. Chem. **6**(7), 470 (2022).
[31]X. Wang, Y. Wang, W. Gao, L. Song, C. Ran, Y. Chen, and W. Huang, Adv. Mater. **33**(12), 2003615 (2021).
[32]D. Di Nuzzo, L. Cui, J. L. Greenfield, B. Zhao, R. H. Friend, and S. C. J. Meskers, ACS Nano **14**(6), 7610 (2020).
[33]Y. Dang, X. Liu, Y. Sun, J. Song, W. Hu, and X. Tao, J. Phys. Chem. Lett. **11**(5), 1689 (2020).
[34]A. Ishii and T. Miyasaka, Sci. Adv. **6**(46), eabd3274 (2020).
[35]J. Ma, C. Fang, C. Chen, L. Jin, J. Wang, S. Wang, J. Tang, and D. Li, ACS Nano **13**(3), 3659 (2019).
[36]C. Chen, L. Gao, W. Gao, C. Ge, X. Du, Z. Li, Y. Yang, G. Niu, and J. Tang, Nat. Commun. **10**(1), 1927 (2019).
[37]B. Zhao, X. Gao, K. Pan, and J. Deng, ACS Nano **15**(4), 7463 (2021).
[38]G. Long, R. Sabatini, M. I. Saidaminov, G. Lakhwani, A. Rasmita, X. Liu, E. H. Sargent, and W. Gao, Nat. Rev. Mater. **5**(6), 423 (2020).
[39]C. Zhang, X. Wang, and L. Qiu, Front. Chem. **9**(543), 711488 (2021).
[40]Z. Liu, C. Zhang, X. Liu, A. Ren, Z. Zhou, C. Qiao, Y. Guan, Y. Fan, F. Hu, and Y. S. Zhao, Adv. Sci. **8**, e2102065 (2021).
[41]H. Ren, Y. Wu, C. Wang, and Y. Yan, J. Phys. Chem. Lett. **12**(10), 2676 (2021).
[42]J. Ahn, S. Ma, J.-Y. Kim, J. Kyhm, W. Yang, J. A. Lim, N. A. Kotov, and J. Moon, J. Am. Chem. Soc. **142**(9), 4206 (2020).
[43]Y. Dong, Y. Zhang, X. Li, Y. Feng, H. Zhang, and J. Xu, Small **15**(39), 1902237 (2019).
[44]J. Ma, H. Wang, and D. Li, Adv. Mater. **33**(26), 2008785 (2021).
[45]G. Long, G. Adamo, J. Tian, M. Klein, H. N. S. Krishnamoorthy, E. Feltri, H. Wang, and C. Soci, Nat. Commun. **13**(1), 1551 (2022).
[46]G. Chen, X. Liu, J. An, S. Wang, X. Zhao, Z. Gu, C. Yuan, X. Xu, J. Bao, H.-S. Hu, J. Li, and X. Wang, Nat. Chem. **15**(11), 1581 (2023).
[47]M.-E. Sun, Y. Wang, F. Wang, J. Feng, L. Wang, H. Gao, G. Chen, J. Gu, Y. Fu, K. Bu, T. Fu, J. Li, X. Lü, L. Jiang, Y. Wu, and S.-Q. Zang, J. Am. Chem. Soc. **145**(16), 8908 (2023).
[48]J.-C. Blancon, J. Even, C. C. Stoumpos, M. G. Kanatzidis, and A. D. Mohite, Nat. Nanotechnol. **15**(12), 969 (2020).
[49]X. Jin, M. Zhou, J. Han, B. Li, T. Zhang, S. Jiang, and P. Duan, Nano Res. **15**, 1047–1053 (2021).
[50]Y.-H. Kim, Y. Zhai, E. A. Gaulding, S. N. Habisreutinger, T. Moot, B. A. Rosales, H. Lu, A. Hazarika, R. Brunecky, L. M. Wheeler, J. J. Berry, M. C. Beard, and J. M. Luther, ACS Nano **14**(7), 8816 (2020).
[51]L.-S. Li, Y.-H. Tan, W.-J. Wei, H.-Q. Gao, Y.-Z. Tang, and X.-B. Han, ACS Appl. Mater. Interfaces **13**(1), 2044 (2021).
[52]M. K. Jana, R. Song, H. Liu, D. R. Khanal, S. M. Janke, R. Zhao, C. Liu, Z. Valy Vardeny, V. Blum, and D. B. Mitzi, Nat. Commun. **11**(1), 4699 (2020).
[53]W. Tao, Q. Zhou, and H. Zhu, Sci. Adv. **6**(47), eabb7132 (2020).
[54]Z. Yuan, C. Zhou, Y. Tian, Y. Shu, J. Messier, J. C. Wang, L. J. van de Burgt, K. Kountouriotis, Y. Xin, E. Holt, K. Schanze, R. Clark, T. Siegrist, and B. Ma, Nat. Commun. **8**(1), 14051 (2017).
[55]Y. Sang, J. Han, T. Zhao, P. Duan, and M. Liu, Adv. Mater. **32**(41), 1900110 (2020).
[56]H. Tanaka, Y. Inoue, and T. Mori, ChemPhotoChem **2**(5), 386 (2018).
[57]J. Wang, C. Fang, J. Ma, S. Wang, L. Jin, W. Li, and D. Li, ACS Nano **13**(8), 9473 (2019).
[58]S. S. Andrews and J. Tretton, J. Chem. Educ. **97**(12), 4370 (2020).
[59]Y. Zheng, J. Xu, and X.-H. Bu, Adv. Opt. Mater. **10**, 2101545 (2021).
[60]W. Chen, S. Zhang, M. Zhou, T. Zhao, X. Qin, X. Liu, M. Liu, and P. Duan, J. Phys. Chem. Lett. **10**(12), 3290 (2019).
[61]H. Ito, H. Sakai, Y. Okayasu, J. Yuasa, T. Mori, and T. Hasobe, Chem. - Eur. J. **24**(63), 16889 (2018).
[62]J. Kumar, T. Nakashima, H. Tsumatori, and T. Kawai, J. Phys. Chem. Lett. **5**(2), 316 (2014).
[63]K. Ma, W. Chen, T. Jiao, X. Jin, Y. Sang, D. Yang, J. Zhou, M. Liu, and P. Duan, Chem. Sci. **10**(28), 6821 (2019).
[64]J. P. Riehl and F. S. Richardson, Chem. Rev. **86**(1), 1–16 (1986).
[65]L. E. MacKenzie, L.-O. Pålsson, D. Parker, A. Beeby, and R. Pal, Nat. Commun. **11**(1), 1676 (2020).
[66]Y. Wang, L. Gao, Y. Yang, Y. Xiang, Z. Chen, Y. Dong, H. Zhou, Z. Cai, G.-C. Wang, and J. Shi, Phys. Rev. Mater. **2**(7), 076002 (2018).
[67]J. Jiang, Z. Chen, Y. Hu, Y. Xiang, L. Zhang, Y. Wang, G.-C. Wang, and J. Shi, Nat. Nanotechnol. **16**(8), 894 (2021).
[68]Q. A. Vu, Y. S. Shin, Y. R. Kim, V. L. Nguyen, W. T. Kang, H. Kim, D. H. Luong, I. M. Lee, K. Lee, D.-S. Ko, J. Heo, S. Park, Y. H. Lee, and W. J. Yu, Nat. Commun. **7**(1), 12725 (2016).
[69]C. Wang, S. K. Behura, and V. Berry, Semicond. Sci. Technol. **35**(7), 075020 (2020).
[70]Y.-H. Kim, Y. Zhai, H. Lu, X. Pan, C. Xiao, E. A. Gaulding, S. P. Harvey, J. J. Berry, Z. V. Vardeny, J. M. Luther, and M. C. Beard, Science **371**(6534), 1129 (2021).
[71]R. Naaman and D. H. Waldeck, J. Phys. Chem. Lett. **3**(16), 2178 (2012).
[72]C.-T. Wang, K. Chen, P. Xu, F. Yeung, H.-S. Kwok, and G. Li, Adv. Funct. Mater. **29**(35), 1903155 (2019).
[73]Z. Fan and A. O. Govorov, Nano Lett. **10**(7), 2580 (2010).
[74]A. H. Jaafar, R. J. Gray, E. Verrelli, M. O'Neill, S. M. Kelly, and N. T. Kemp, Nanoscale **9**(43), 17091 (2017).
[75]A. Sengupta and K. Roy, Appl. Phys. Rev. **4**(4), 041105 (2017).